

Supporting Information

Measuring Cellular Ion Transport by Magnetoencephalography

Sudhir Kumar Sharma,[†] Sauparnika Vijay,[‡] Sangram Gore,[‡] Timothy M. Dore,^{‡§*}
and Ramesh Jagannathan^{†*}

[†]Engineering Division, New York University Abu Dhabi, United Arab Emirates

[‡]Science Division, New York University Abu Dhabi, United Arab Emirates

[§]Department of Chemistry, University of Georgia, Athens, Georgia 30602, United States of America

Table of Contents

Figure S1: Screen shot of noise reduced data shown in Figure 2e.

Figure S2: Overlaid plots of data shown in Figure 2e.

Figure S3: Impact of adding culture media remotely to the cell flask.

Figure S4: Cell viability results as a function of dosage level of capsaicin, effect of addition of capsaicin (10 μ M final concentration) at time ($t = 30$ s) to HEK293 cells expressing TRPV1 channels, effect of addition of capsaicin (10 μ M final concentration) at time ($t = 24$ s) to HEK293 cells expressing TRPV1 channels with TRPV1 antagonist (10 μ M ruthenium red).

Figure S5: Verification of TRPV1 (MW = 93-95 kDa) expression in stably transfected HEK 293 cells.

Figure S6: Overlaid plots of data shown in Fig, 3e.

Figure S7: Effect of increasing capsaicin concentration on the measured magnetic field from TRPV1-expressing HEK293 cells.

Figure S8: Addition of culture media without capsaicin remotely to the cell flask.

Figure S9: Confocal fluorescence experimental data on the effect of multiple additions of capsaicin to the same TRPV1-expressing HEK293 cells.

Figure S10: MEG noise reduced data on the effect of multiple additions of capsaicin to the same HEK293 cells expressing TRPV1 channels.

Figure S11: Confocal fluorescence experimental data on the effect of replacing the culture media before the second capsaicin addition, by washing the with fresh culture media three times.

Figure S12: MEG data on the effect of replacing the culture media before the second capsaicin addition, by washing the TRPV1-expressing HEK293 cells with fresh culture media three times.

Figure S13: Screen shot of the MEG noise reduced data shown in Fig. 4a.

Figure S14: Overlaid plots of data shown in Fig. 4a.

Figure S15: FFT of the data of channel 175 shown in Figure 4a.

Figure S16: Screen shot of the MEG noise reduced signals from the control experiment data shown in Fig.4b.

Figure S17: Magnetic fields from HeLa cells dispersed in culture

Figure S18: Morphological characterization of H9c2(2-1) cells before and after differentiation.

Figure S19: Comparison of the magnetic signals from non-differentiated and differentiated cardiac cells.

Figure S1:

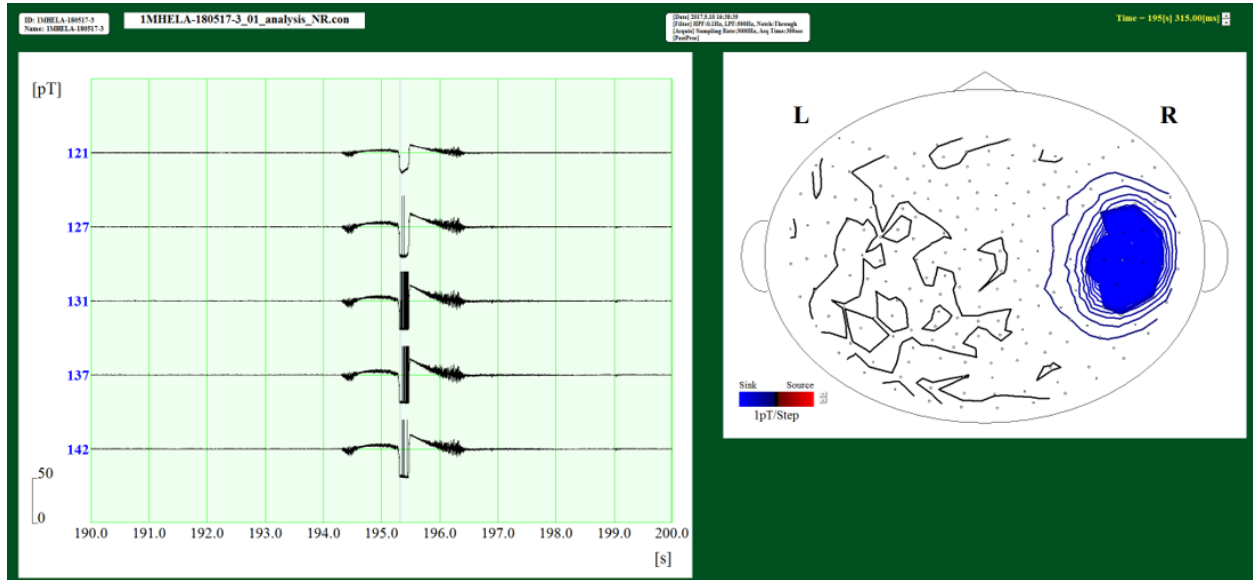


Figure S1: Screen shot of noise reduced data shown in Figure 2e.

Figure S2:

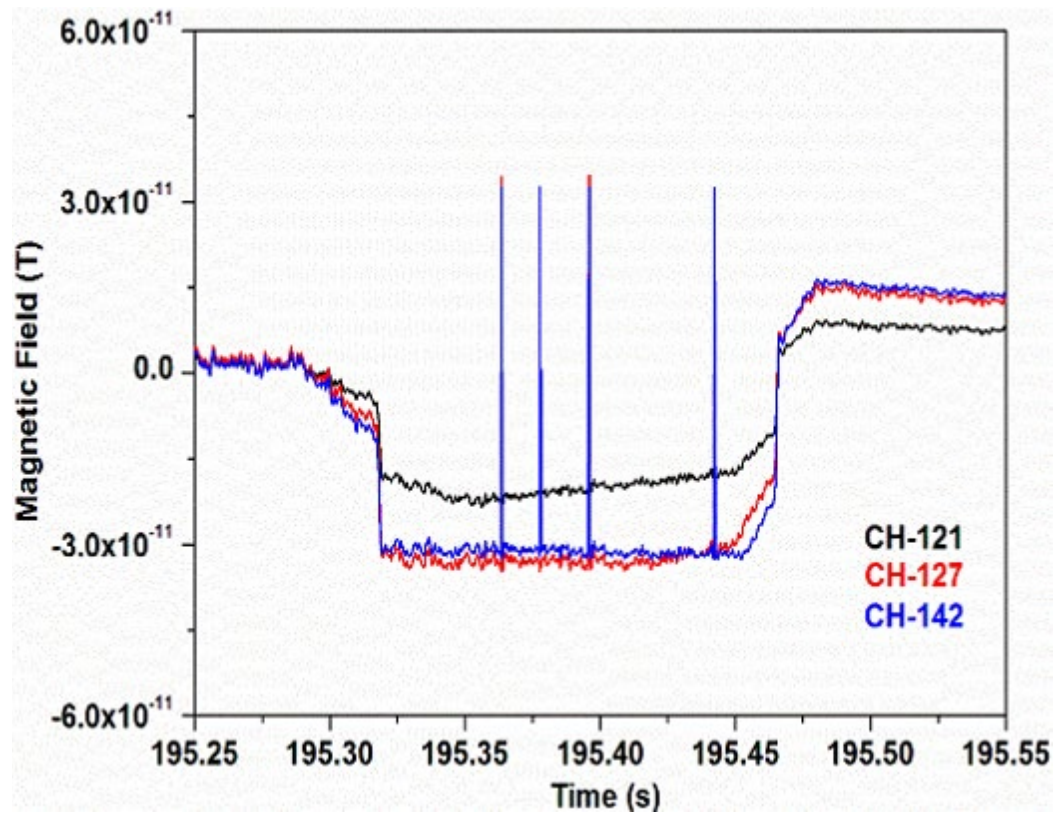


Figure S2: Overlaid plots of data shown in Figure 2e.

Figure S3:

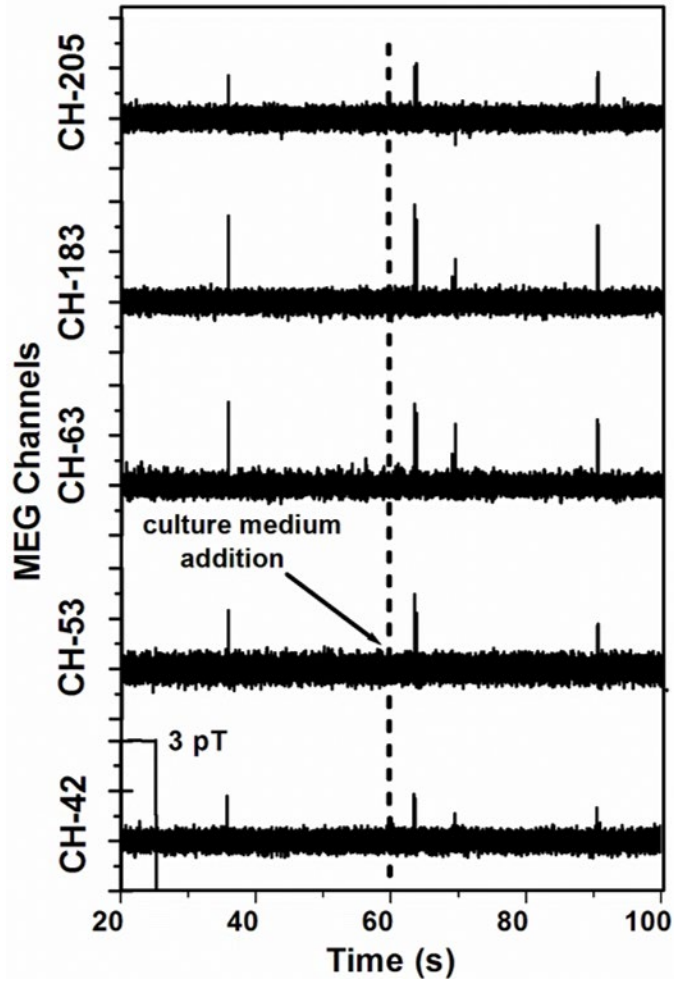


Figure S3: Impact of adding culture media remotely to the cell flask.

Figure S4:

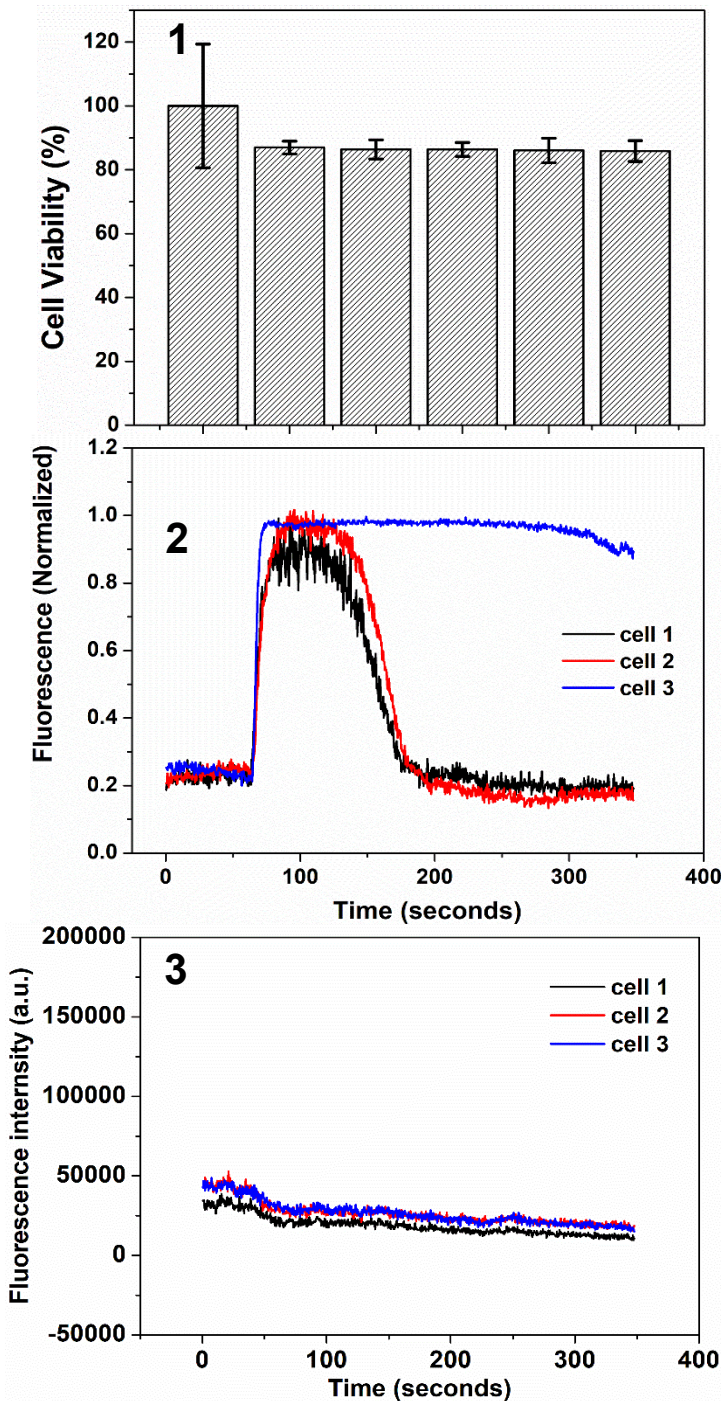


Figure S4: (1) Cell viability results as a function of dosage level of capsaicin (2) Effect of addition of capsaicin ($10 \mu\text{M}$ final concentration) at time ($t = 30 \text{ s}$) to HEK293 cells expressing TRPV1 channels. (3) Effect of addition of capsaicin ($10 \mu\text{M}$ final concentration) at time ($t = 24 \text{ s}$) to HEK293 cells expressing TRPV1 channels with TRPV1 antagonist ($10 \mu\text{M}$ ruthenium red).

Figure S5:

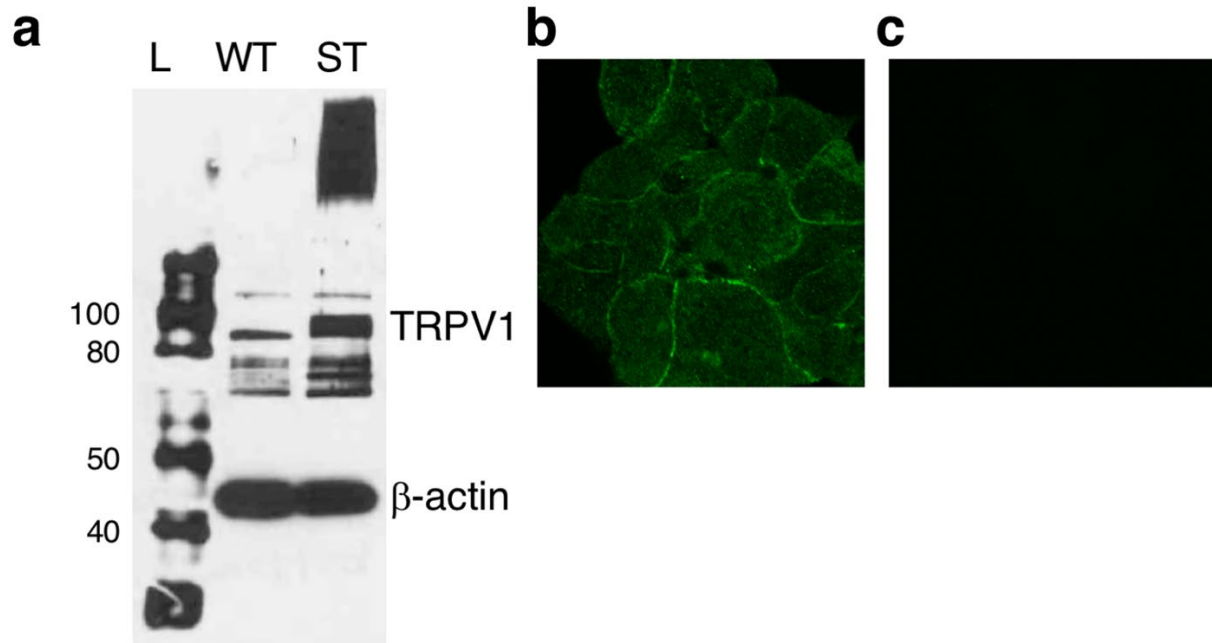


Figure S5: Verification of TRPV1 (MW = 93-95 kDa) expression in stably transfected HEK 293 cells. (a) Western blot analysis of wild type (WT) and stably transfected (ST) cells and a molecular weight ladder (L): protein extracts were loaded on 10% SDS polyacrylamide gels, then the nitrocellulose membranes were split at the position of proteins of 40 kDa. The antibodies used and their dilutions were anti-TRPV1 (1:500, rabbit polyclonal, Origene, cat. #TA309921), anti-biotin (1:1,000, HRP linked), and anti-rabbit-HRP (1:2,000, goat secondary). β -Actin protein (MW = 42 kDa) was used as a control. (b and c) Immunofluorescence staining of HEK 293(TRPV1) cells treated (b) with TRPV1 specific antibody (anti-TRPV1, 1:250; secondary antibody, 1:500) and (c) without primary antibody.

Figure S6:

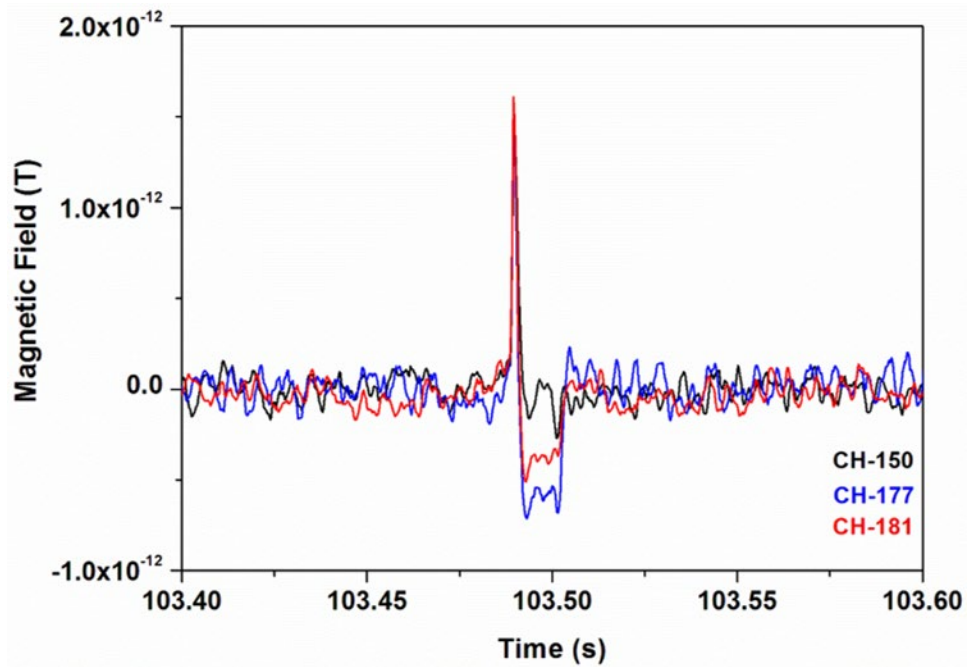


Figure S6: Overlaid plots of data shown in Fig. 3e.

Figure S7:

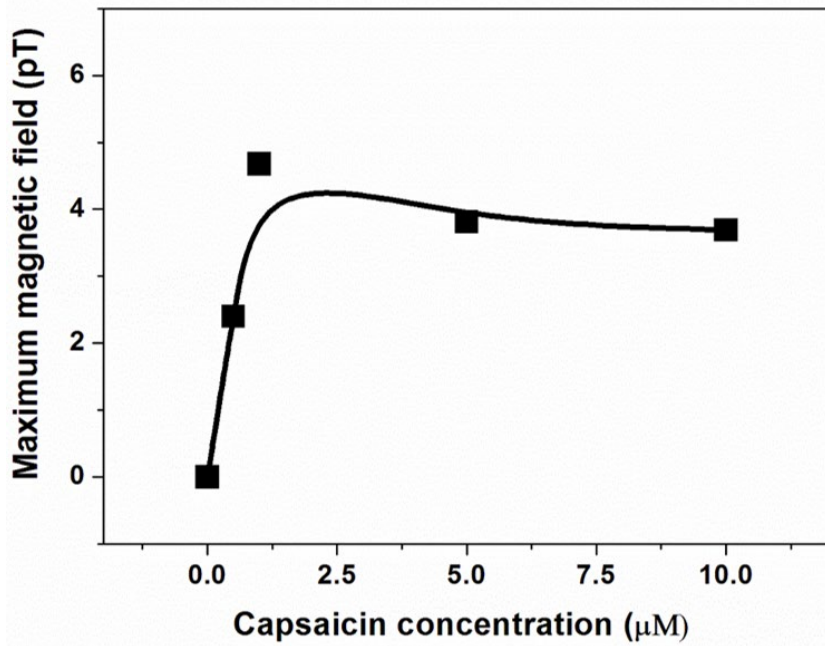


Figure S7: Effect of increasing capsaicin concentration on the measured magnetic field from TRPV1-expressing HEK293 cells.

Figure S8:

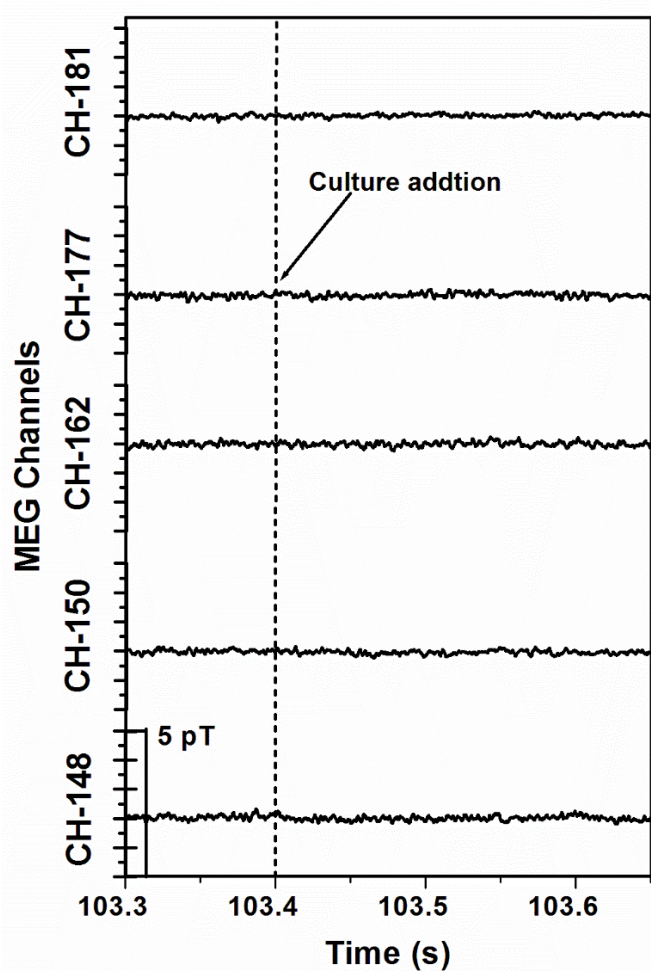


Figure S8: Addition of culture media without capsaicin remotely to the cell flask.

Figure S9:

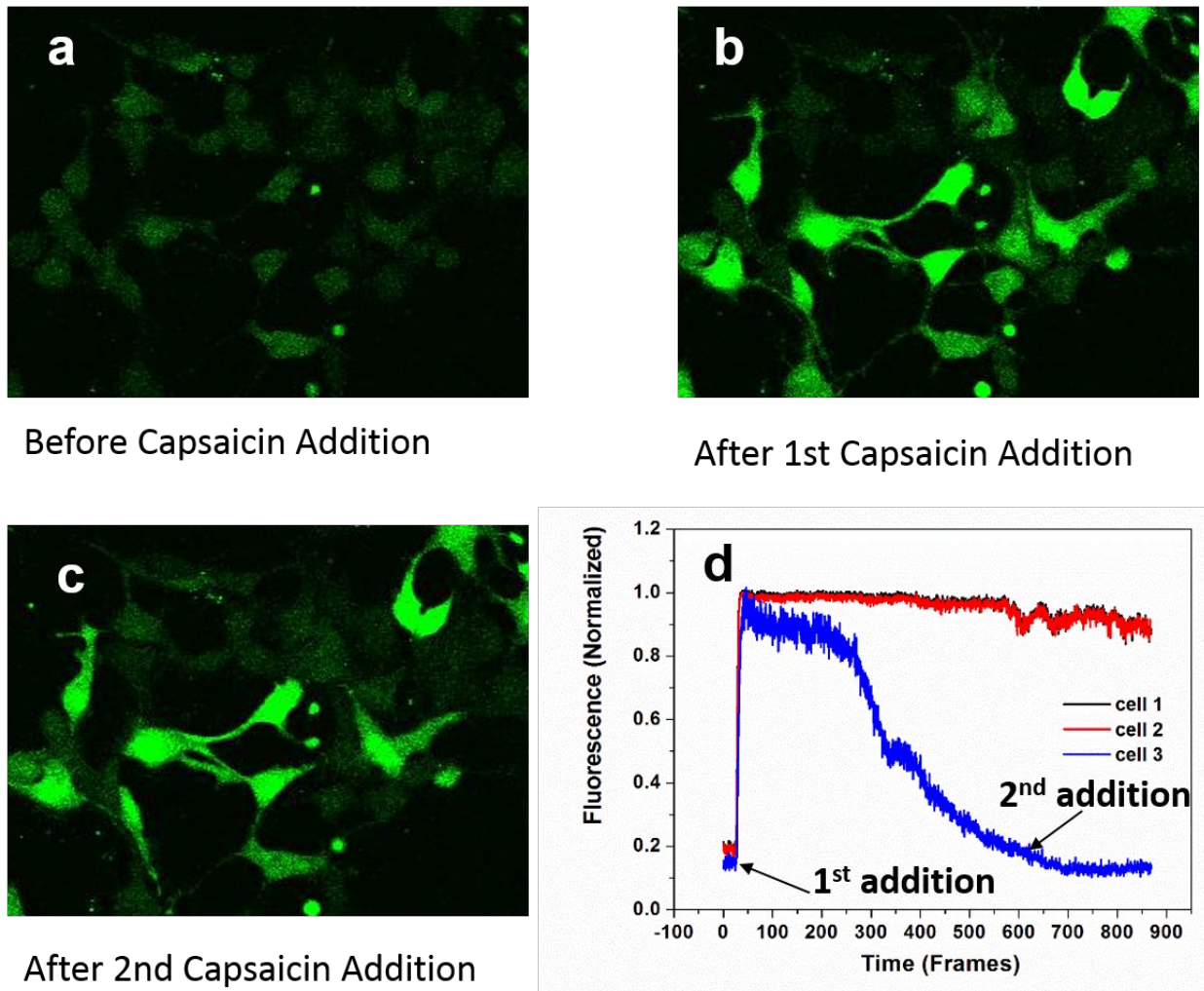


Figure S9: Confocal fluorescence experimental data on the effect of multiple additions of capsaicin to the same TRPV1-expressing HEK293 cells: (a) before capsaicin addition, (b) after capsaicin addition, (c) after second capsaicin addition, (d) fluorescence (normalized) as a function of time, after the first capsaicin addition and after the second capsaicin addition.

Figure S10:

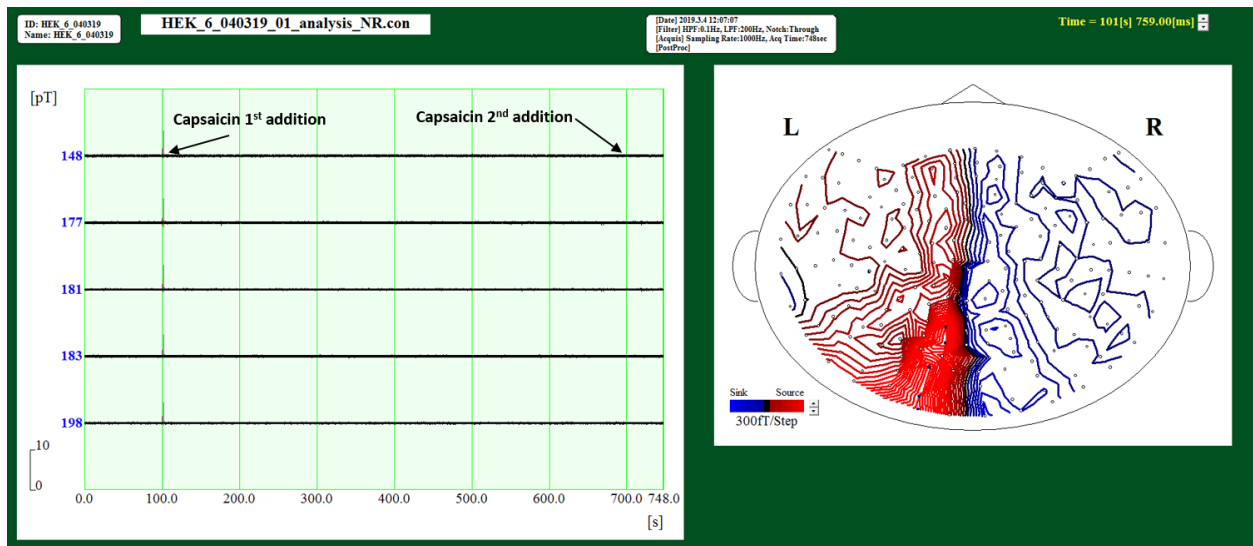


Figure S10: MEG noise reduced data on the effect of multiple additions of capsaicin to the same HEK293 cells expressing TRPV1 channels.

Figure S11:

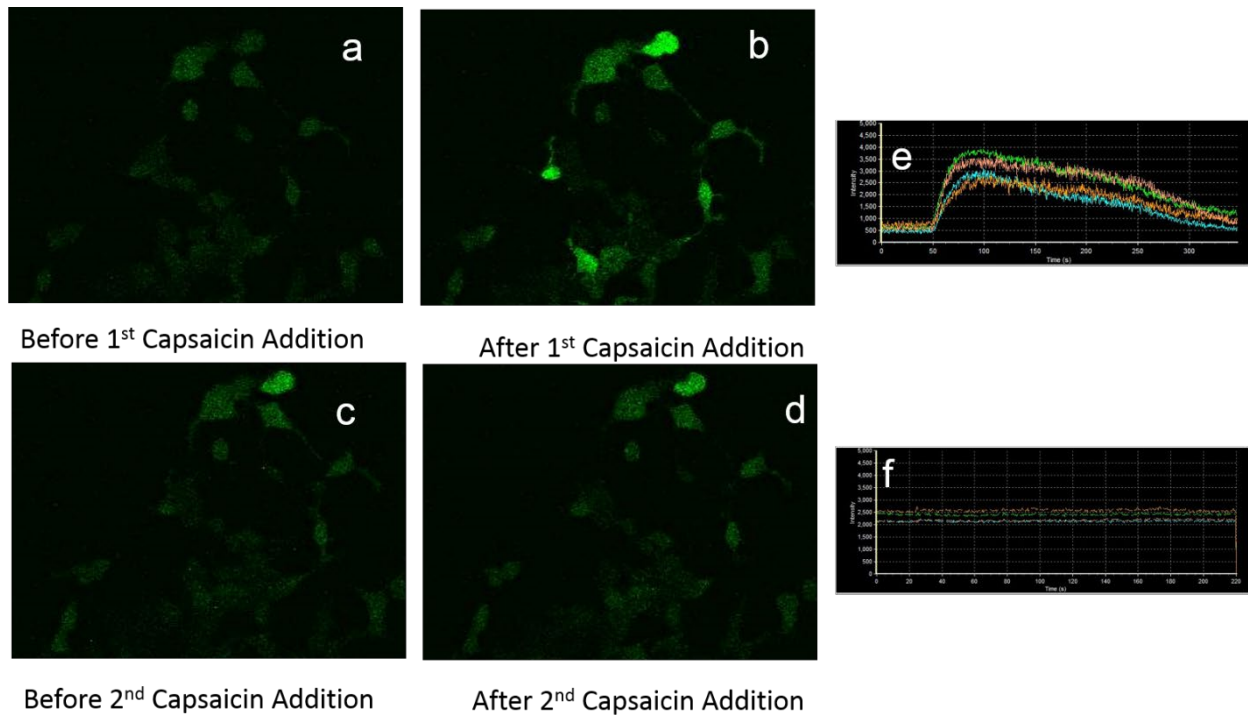


Figure S11: Confocal fluorescence experimental data on the effect of replacing the culture media before the second capsaicin addition, by washing the with fresh culture media three times: (a) before first capsaicin addition, (b) after first capsaicin addition, (c) before second capsaicin addition, (d) after second capsaicin addition, (e) fluorescence intensity vs time after first addition (screen shot), (f) fluorescence vs time after second addition (screen shot).

Figure S12:

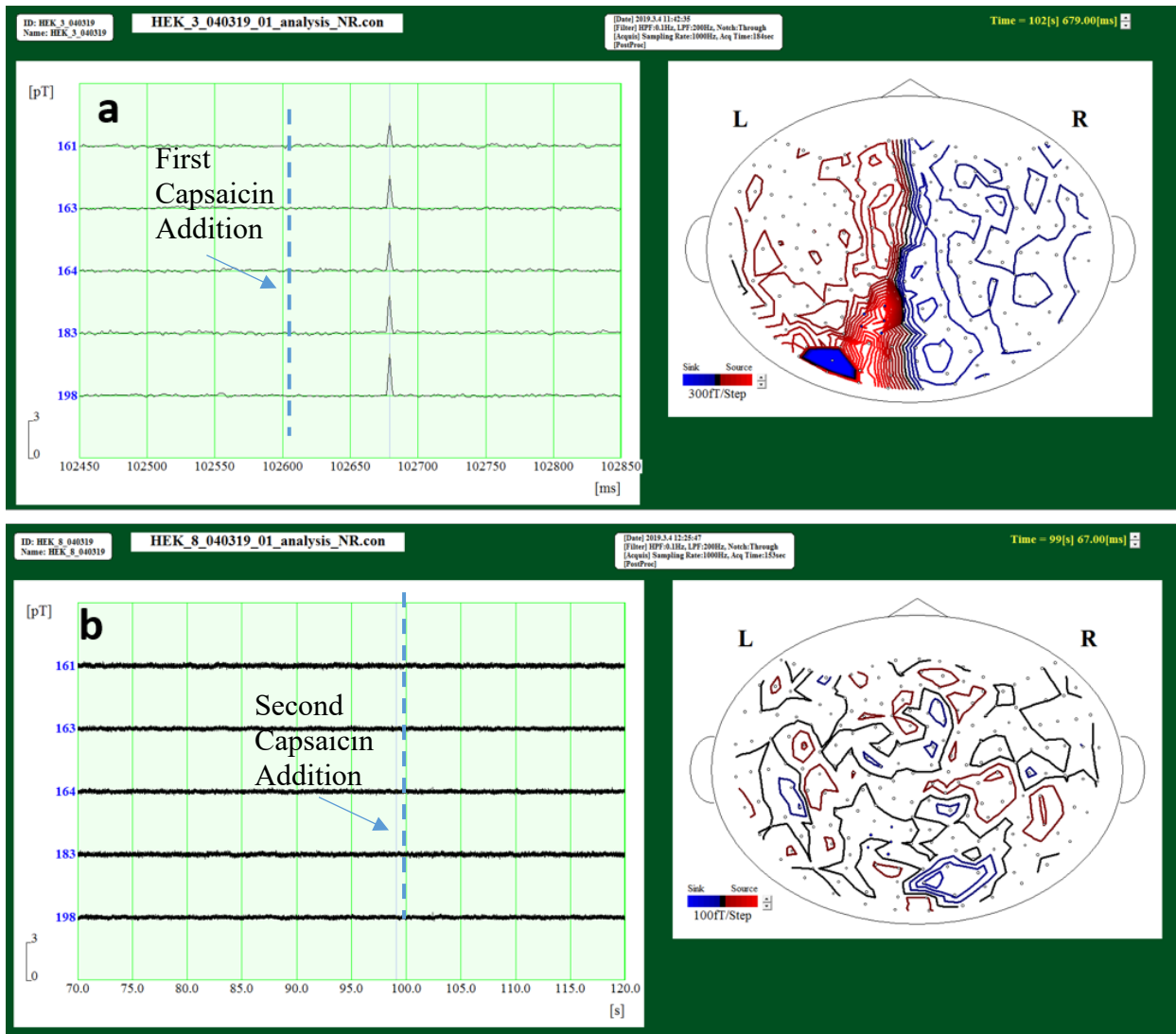


Figure S12: MEG data on the effect of replacing the culture media before the second capsaicin addition, by washing the TRPV1-expressing HEK293 cells with fresh culture media three times. a) Screen shot of the noise reduced data for first capsaicin addition. b) Screen shot of noise reduced data for the second capsaicin addition.

Figure S13:

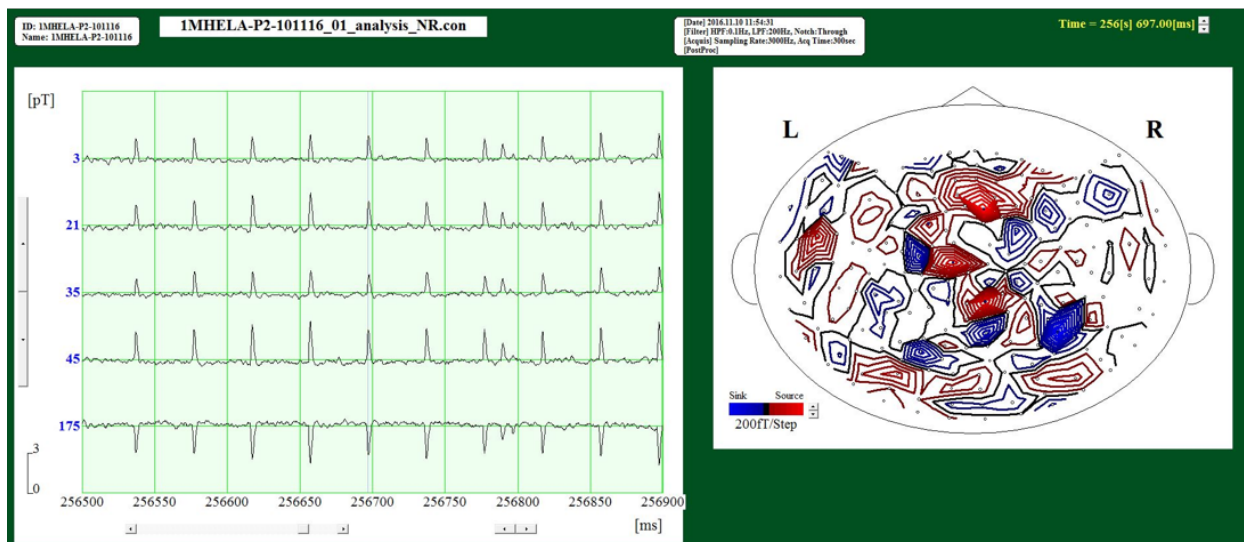


Figure S13: Screen shot of the MEG noise reduced data shown in Fig. 4a.

Figure S14:

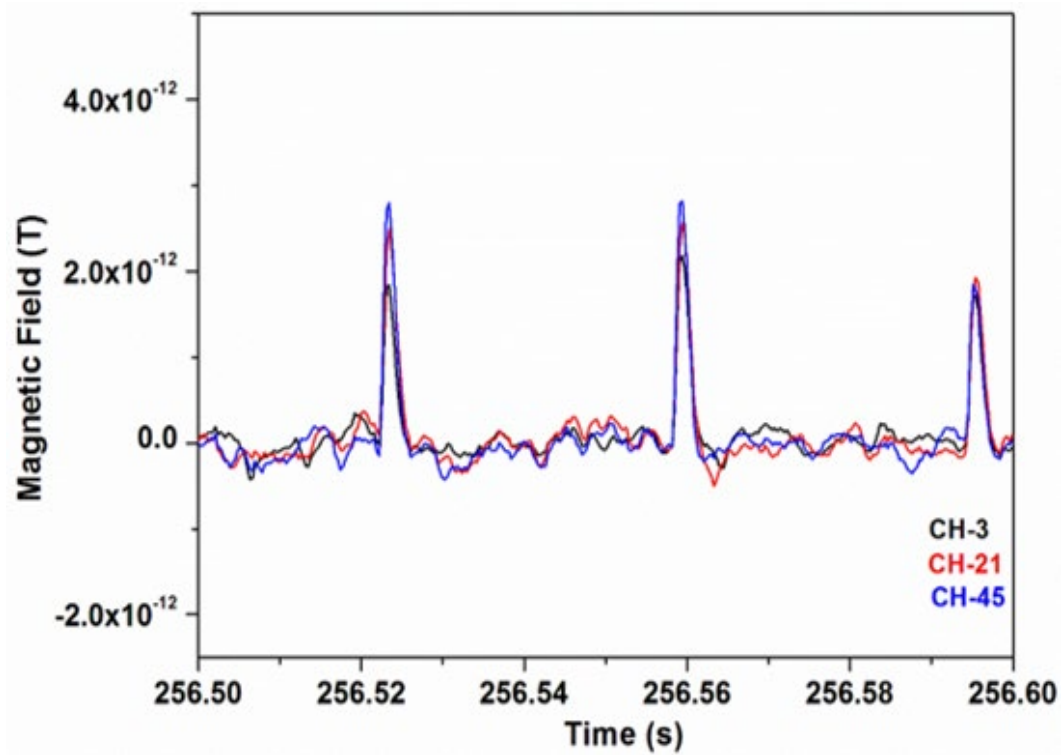


Figure S14: Overlaid plots of data shown in Fig. 4a.

Figure S15:

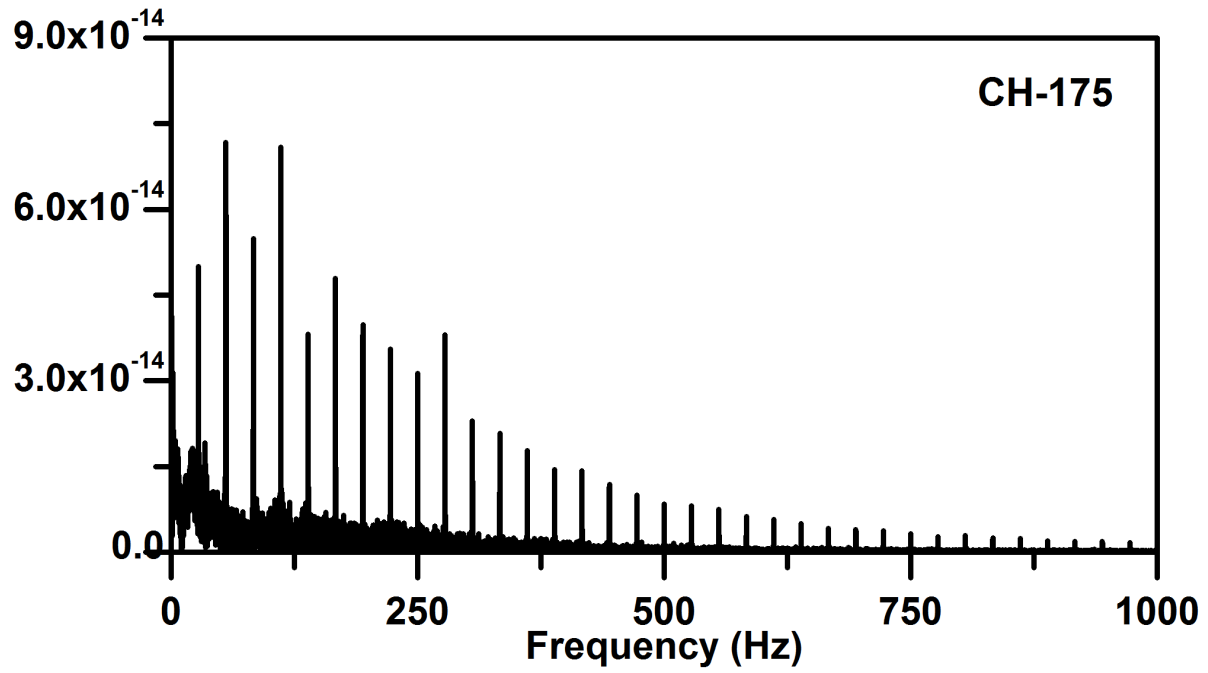


Figure S15: FFT of the data of channel 175 shown in Figure 4a.

Figure S16:

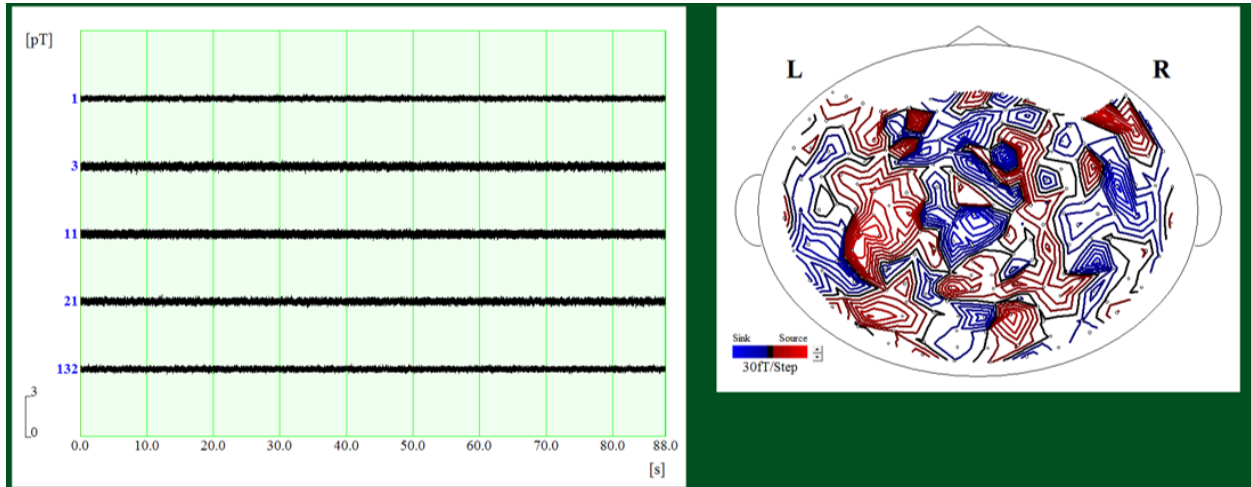


Figure S16: Screen shot of the MEG noise reduced signals from the control experiment data shown in Fig.4b.

Figure S17:

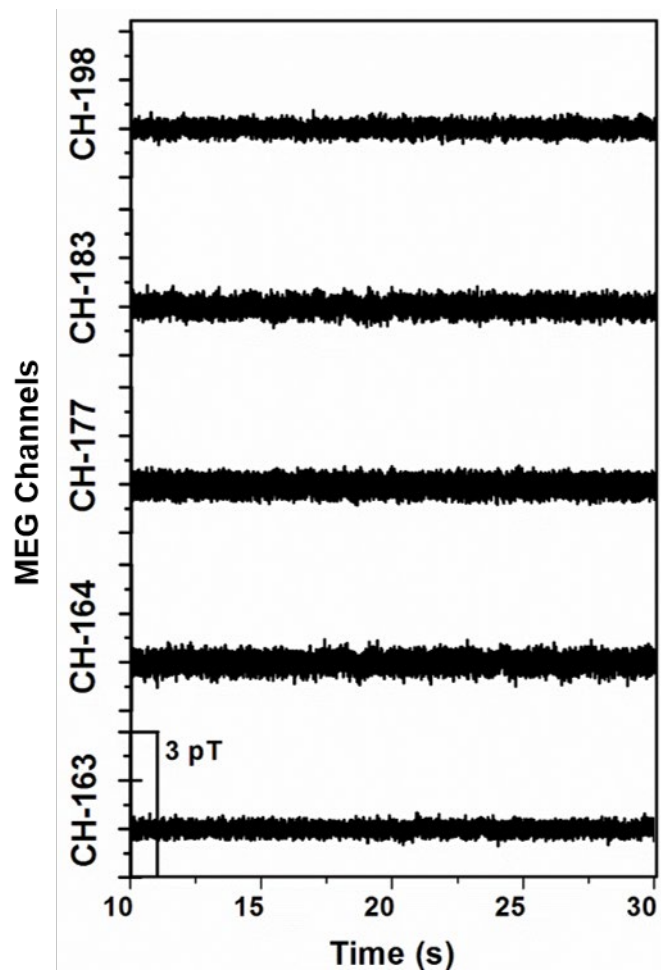


Figure S17: Magnetic fields from HeLa cells dispersed in culture.

Figure S18:

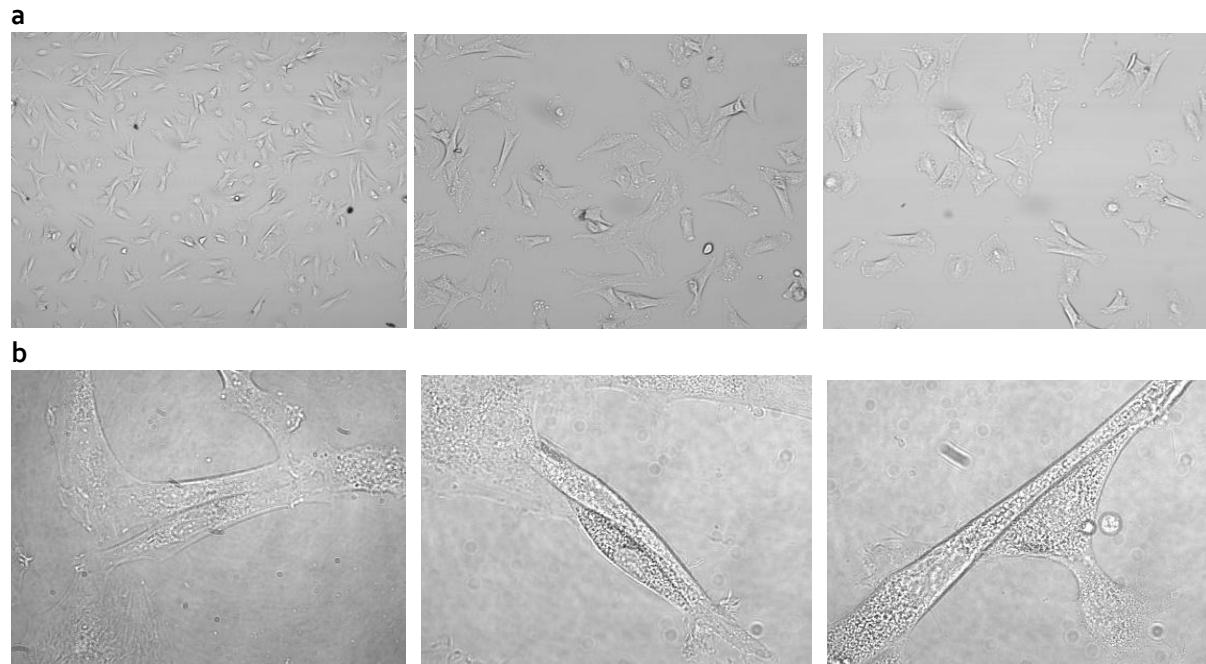


Figure S18: Morphological characterization of H9c2(2-1) cells before and after differentiation. (a) Representative images of non-differentiated H9c2(2-1) cells grown in 10% FBS media showing the characteristic stellar shape of myoblasts. (b) Representative images of H9c2(2-1) cells after five days of differentiation in low serum media (2% FBS) showing the characteristic elongated shape of myocytes.

Figure S19:

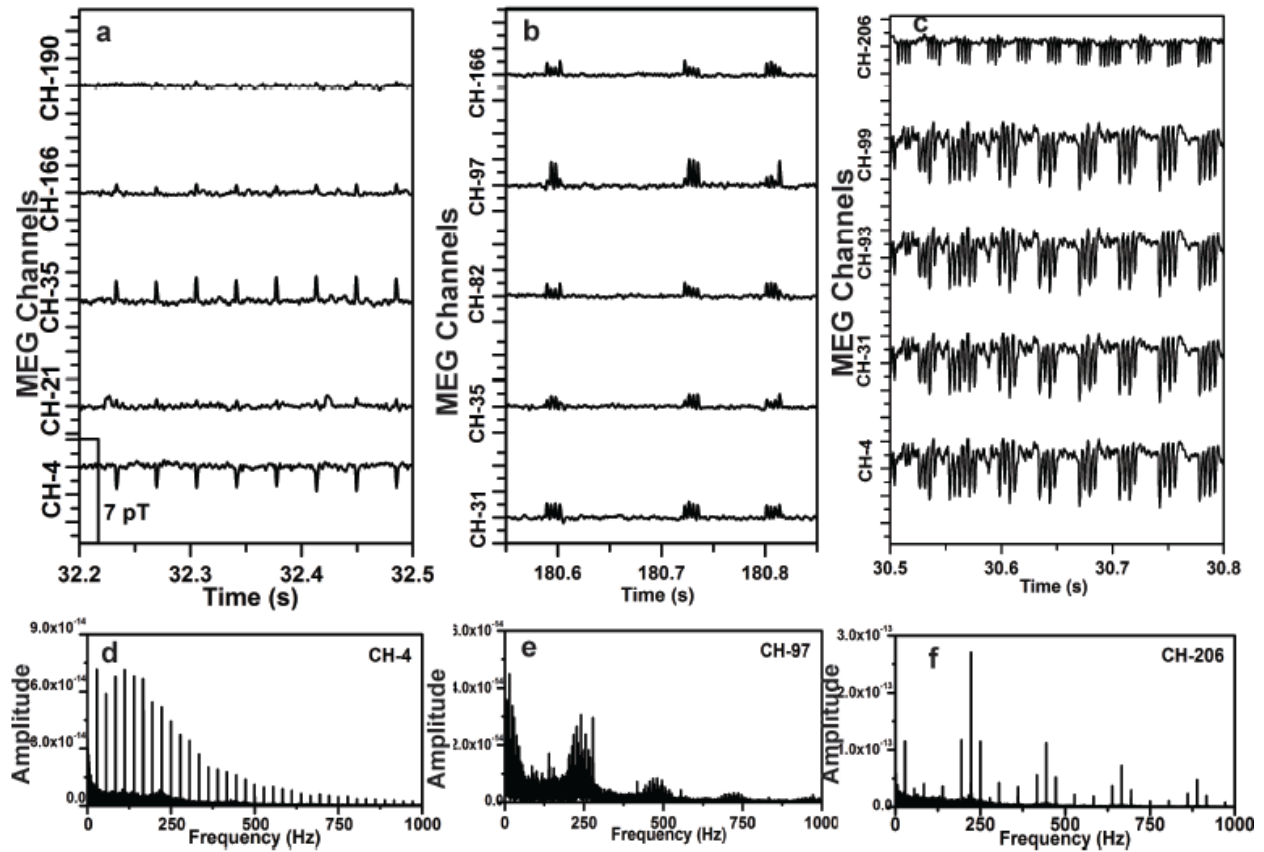


Figure S19: Comparison of the magnetic signals from non-differentiated and differentiated cardiac cells. (a) Data for 1×10^6 H9c2(2-1) rat cardiac myoblasts detected by channels 4, 21, 35, 166, and 190. (b and c) Data for 1×10^6 H9c2(2-1) rat cardiac cells differentiated into myocytes detected by channels 31, 35, 82, 97, and 166 and 4, 31, 93, 99, and 206. (d) FFT of the data for non-differentiated cells (channel 4). (e and f) FFT of the data for differentiated cells (channels 97 and 206).